Cell. Mol. Biol. (ISSN: 1165-158X)

Journal Homepage: www.cellmolbiol.org

Cellular and Molecular Biology

Original Article

Myoblast-derived exosomes reduce anticancer drug-induced muscle toxicity via an autocrine pathway

Woojin Lee, Euijin Sohn, Sang Bum Kim*

College of Pharmacy, Sahmyook University, Seoul, Republic of Korea 01795

Article Info

Article history:

Received: March 21, 2024
Accepted: June 23, 2024
Published: October 31, 2024

Use your device to scan and read the article online

Abstract

During cancer treatment, cachexia, characterized by muscle loss, often occurs, with one of the contributing factors being muscle toxicity caused by anticancer drugs. It affects approximately 80% of patients with cancer, particularly those with digestive organ malignancies. However, effective treatment for this condition remains elusive. Therefore, in this study, we aimed to investigate the therapeutic potential of exosomes in relieving cachexia. Specifically, we examined the exosomes derived from muscle stem cells, which are involved in muscle cell regeneration and their role in controlling anticancer drug-induced muscle toxicity. First, exosomes secreted from myoblasts under depletion conditions were characterized. Exosomes were isolated under serum starvation conditions, displaying an average size of 113 nm and containing typical exosome marker proteins. Furthermore, electron microscopy confirmed their exosomal nature. To confirm the paracrine function of myoblast-derived exosomes (MDEs), a significant increase in cell viability was observed upon their application to myoblasts. No changes were observed in the cell cycle during exosome treatment. However, it was confirmed that the quantity of viable cells increased under serum starvation conditions. This suggests that MDEs possess the function of enhancing myoblast survival and overall cell viability. Cachexia, a prevalent condition in patients with cancer, often manifests as muscle cell depletion induced by anticancer drugs. The potential of MDEs to inhibit cell death induced by anticancer drugs was investigated. The findings revealed that while high concentrations of oxaliplatin and doxorubicin, known to induce cachexia, did not restore cell viability, lower concentrations did. This study suggests that MDEs may have the potential to control cachexia, a common side effect of anticancer drugs, by reducing muscle cell damage induced by anticancer drugs.

Keywords: Doxorubicin, Exosome, Muscle toxicity, Myoblasts, Oxaliplatin.

1. Introduction

Cancer cachexia, a complex metabolic syndrome, causes continuous weight, and muscle loss. [1] Approximately half of all patients with cancer experience cachexia, resulting in death in 22% of them. [2, 3] Furthermore, it impairs chemotherapy effectiveness and exacerbates side effects [4, 5] In this condition, muscle atrophy directly correlates with mortality. [6] The direct causes of muscle atrophy are inflammatory cytokines and muscle-specific protein degradation. [6, 7] Chemotherapy induces muscle consumption. [8] Moreover, anticancer drugs are directly toxic to muscles, leading to muscle loss and dysfunction.

Chemotherapy is a well-established treatment for various cancer conditions. [9] Doxorubicin (DOX), classified as an anthracycline, is used as a cell proliferation inhibitor in treating blood, breast, and various solid tumors. [10] Its anticancer mechanism involves strong binding to the cell nucleus and subsequent insertion into deoxyribonucleic acid (DNA), forming a DOX-DNA complex that induces cell apoptosis. [11-13] Oxaliplatin (OXA), a third-generation platinum complex, is currently used to treat solid cancers, such as colorectal and advanced ovarian cancer. [14, 15] Activated OXA generates platinum-DNA adducts containing bulky 1,2-diaminocyclohexane rings, effectively inhibiting DNA replication and demonstrating anticancer activity. [15, 16] However, these drugs negatively affect other cells, resulting in adverse effects that induce apoptosis. [10, 12, 13, 15, 17, 18] Moreover, these anticancer drugs induce muscle toxicity, leading to muscle loss and functional impairments. [19-23] This muscle loss, attributed to toxicity, hampers the continued administration of anticancer drugs, thus negatively affecting patient survival rates. [6, 24-26] Although the specific mechanism of muscle loss remains incompletely identified, muscle regeneration begins with myoblasts after muscle loss. The key mechanism for damaged muscle self-renewal cells involves the proliferation of myoblasts and their subsequent differentiation into myotubes. However, research investigating the mechanism protecting myoblasts from the adverse effects of anticancer drugs is currently inadequate. Recent studies indicate that dying cells possess protective mechanisms that extend to neighboring cells. [13] Skeletal muscles employ a repair mechanism after injury, wherein satellite cells are activated, differentiate into myoblasts, and rapidly proliferate to fuse with damaged muscle fibers. This process is also modulated by exosomes. [25, 27-29]

* Corresponding author.
E-mail address: sbk@syu.ac.kr (S. B. Kim).
Doi: http://dx.doi.org/10.14715/cmb/2024.70.10.15

Exosomes, ranging from 30 to 150 nm in size and enclosed by a lipid bilayer, are extracellular vesicles discharged from cells. [30] They contain DNA, RNA, and proteins, which they release into the extracellular environment, enabling interactions with surrounding cells and playing a vital role in intercellular communication. [31-34] Exosomes promote the proliferation and differentiation of target cells. [35] Previous studies have shown that exosomes also regulate the survival of parent cells. For example, they exert control over cancer cell growth and metastasis. [36, 37] Owing to their biocompatibility and capacity as carriers, exosomes hold potential in molecular therapeutics for cell protection. [38, 39] Therefore, this study aims to investigate how exosomes released from myoblasts under cell death conditions, especially serum starvation, can protect muscle cells from drugs and cell death. [40]

This study demonstrated the restoration of myoblast viability during serum starvation, a condition associated with myoblast death, using myoblast-derived exosomes (MDEs). Subsequently, the exosome protein profile was determined using mass spectrometry to confirm their potential cell death inhibitory function. After identifying the protein IDs in the exosomes, Gene Ontology (GO) analysis was conducted to understand their functional roles. Furthermore, the therapeutic potential of MDEs in inhibiting cachexia induced by DOX and OXA, two anticancer drugs known to cause cachexia, was assessed.

2. Materials and methods

2.1. Cell culture

C2C12 myoblast cells were purchased from the American Type Culture Collection (ATCC). They were cultured in HyClone™ Dulbecco's Modified Eagle Medium/High glucose (DMEM, Hyclone), supplemented with 10% heat-inactivated Fetal Bovine Serum (FBS; Hyclone) and 1% penicillin/streptomycin (P/S;s Gibco / COM). The cell culture was incubated at 37°C in an incubator (ICU 240 Eco, Memmert) with a 5% carbon dioxide environment.

2.2. Exosome purification

The cells were grown to approximately 80% density, after which the medium was replaced with DMEM containing 1% P/S and cultured for 24 h. Subsequently, the supernatant was collected and centrifuged at 1,000 RCF for 10 min at 4℃ to eliminate dead cells and debris. The resulting supernatant was harvested again and centrifuged at 10,000 RCF for 35 min at 4℃ to eliminate cell fragments and large vesicles produced during cell death. The supernatant underwent further concentration by filtration through a 100 kDa Amicon filter (Merck), followed by ultracentrifugation at 100,000 RCF for 1 h and 10 min at 4℃. The precipitate was then resuspended in DMEM. Protein quantity was determined using a BCA Protein Assay Kit (Thermo Fisher Scientific) before use.

2.3. Nanoparticle Tracking Analysis (NTA)

The extracted exosomes were diluted in 1 mL of distilled water (DW), and their particle size was measured with the Nanosight NS300 system (Malvern). Data analysis was performed using NTA software (version 3.2).

2.4. Transmission Electron Microscopy

(A) [TEM image processing]

To capture negatively stained electron microscopy images, 5 μl of each purified sample was administered onto carbon-coated grids, which underwent a 1-minute glow-discharge treatment (Harrick Plasma) in ambient air. Following this, the grids were subjected to negative staining using a 1% uranyl acetate solution. The resultant prepared grids were examined using a Tecnai 10 transmission electron microscope outfitted with a Lanthanum hexaboride (LaB¬6, FEI) cathode, operated at 100 kV. Images were documented using a 2Kx2K UltraScan CCD camera (Gatan) at a magnification of 10,000 (equivalent to 1.0 nm per pixel). This equipment setup was situated at the Kangwon Center for Systems Imaging in Chuncheon, Republic of Korea. [41]

(B) [Cryo-EM data collection and sample preparation]

For cryo-EM, 4 μl of each prepared sample was applied to glow-discharged Quantifoil R 1.2/1.3 300 mesh holey carbon EM grids (Quantifoil) using a Vitrobot Mark IV (Thermo Fisher), with a 4-second blotting time and 100% humidity at 4°C. The prepared grids were then transferred to an Elsa Cryo-Transfer Holder 698 (Gatan). Subsequently, they were examined using a Tecnai 10 TEM (FEI) at 100 kV, with temperature monitoring. Images were captured using an UltraScan CCD camera (Gatan) at a nominal magnification of 40,000×. These instruments were housed at the Kangwon Center for Systems Imaging in Chuncheon, Republic of Korea. [41]

2.5. DIL Staining

A culture medium was prepared by adding 1,1'-dioctadecyl-3,3,3',3'-tetramethylindocarbocyanine perchlorate (DIL) to DMEM containing 1% P/S at a concentration of 100 nM/ml. Cells were cultured to 80% confluence, at which point the supernatant was aspirated and replaced with the DIL-mixed medium. After 24 h of culture, the supernatant was collected and centrifuged at 1,000 RCF for 10 min at 4℃. This resulted in the isolation of only the supernatant. The supernatant was centrifuged at 10,000 RCF for 35 min at 4℃, filtered using a 100 kDa Amicon filter (Merck) for concentration, and subsequently ultracentrifuged at 100,000 RCF for 1 h and 10 min. The precipitate was used to treat the cells, which were subsequently observed under a fluorescence microscope.

2.6. Cell viability assay

To assess the effects of exosomes extracted from C2C12 myoblasts on muscle cells and the toxicity of DOX and OXA, C2C12 myoblasts were plated in a 96-well plate at a density of 1 x 10^4 cells/well and incubated in a CO2 incubator for 24 h. After supernatant removal, exosomes were added to DMEM with 1% P/S and COM at a concentration of 20 μg/mL. To investigate the effect of exosomes on the toxicity of Doxorubicin hydrochloride (44583-10MG, Sigma) and Oxaliplatin (O9512-5MG, Sigma) on muscle cells, the compounds were mixed with exosomes at concentrations of 1 μM, 0.8 μM, and 20 μg/ml respectively, adjusting the total volume to 200 μL for 24 h of incubation. After supernatant removal, 10 μL of Cell Counting Kit-8 (CCK, Dojindo) was added to 90 μL of DMEM containing 1% P/S in each well. Absorbance was subsequently measured at a wavelength of 450 nm using a microplate reader (SpectraMax ABS, Molecular Devices).

2.7. Cell cycle Analysis and cell count

To determine the effect of exosomes extracted from

C2C12 myoblasts on cell proliferation, C2C12 myoblasts were plated at 1 x 10^5 cells/well in 6-well plates and incubated in a CO2 incubator for 24 h. After supernatant removal, the cells were treated with exosomes at a concentration of 20 µg/mL, followed by a 24-h incubation period. The cells were subsequently washed with PBS, harvested, and diluted 1:1 (v:v) with trypan blue for cell counting using a Countess™3 (Thermo Fisher). The remaining cells were then fixed in 70% ethanol at -4°C for 24 h. The cells were stained with FxCycle™ PI/RNase Staining Solution (Thermo Fisher) and subjected to cell cycle analysis using a CytoFLEX flow cytometer (Beckman Coulter).

2.8. Western blotting

C2C12 myoblasts were cultured at a density of 1.5 x 10^5 cells in a 6-well plate for 24 h. After supernatant removal and three washes with PBS, the cells were lysed in Radio-Immunoprecipitation Assay (RIPA) buffer at 4°C for 15 min. Subsequently, they were centrifuged at 18,000 RCF for 15 min at 4°C. Finally, 30 µg of protein was mixed with 5X Tris-glycine sample buffer (SB) using the BCA kit. For exosome analysis, 30 µg of total protein extracted from exosomes was mixed with SB and boiled at 100°C for 15 min to prepare samples. These samples were then loaded onto a 10% sodium dodecyl sulfate–polyacrylamide (SDS) gel for electrophoresis. After electrophoresis, the proteins were transferred to an Immobilon®-P PVDF Membrane 0.45 µM (Thermo Fisher Scientific) and blocked at room temperature for 1 h in a solution containing 5% skim milk, Tris-Buffered Saline, and 0.2% tween20 (TBST). Subsequently, the membrane was incubated overnight at 4°C with primary antibodies Tumor Susceptibility Gene 101 (TSG101), apoptosis-linked gene 2-interacting protein X (Alix), heat shock protein 70 (HSP70) at a 1:1000 ratio in TBST with 1% skim milk. The membrane underwent three 5-min washes with TBST. It was then incubated for 1 h at room temperature with a secondary antibody at a 1:10000 ratio in 1 % skim milk. After three more washes, the membrane was treated with an Enhanced Chemiluminescence (ECL) solution (Absignal), prepared by mixing reagents A and B in a 1:1 ratio, and analyzed using a WSE-6200 LuminoGraph II (ATTO).

2.9. RP-nano LC-ESI-MS/MS analysis

An analysis was performed using a Thermo Scientific Quadrupole-Orbitrap instrument (Thermo Fisher Scientific) coupled with a Dionex U 3000 RSLCnano HPLC system. Mass spectrometry analyses were conducted using a Thermo Scientific Orbitrap Exploris 240 mass spectrometer.

Fractions were reconstituted in solvent A (water/acetonitrile, 98:2 v/v, with 0.1% formic acid) before being injected into the LC-nano ESI-MS/MS system. The samples underwent initial trapping on an Acclaim PepMap 100 trap column (100 µm x2 cm, nanoViper C18, 5 µm, 100 Å, Thermo Fisher Scientific, part number 164564). They were washed for 6 min with 98% solvent A (water/acetonitrile, 98:2 v/v, with 0.1% formic acid) at a flow rate of 4 µL/min. Subsequently, they were separated on a PepMap RSLC C18 column (75 µm x 15 cm, nanoViper C18, 3 µm, 100 Å, Thermo Fisher, part number ES900) at a flow rate of 300 nL/min.

The LC gradient began at 2% solvent B and increased to 8% over 10 min, then from 8% to 30% over 55 min. This was followed by 90% solvent B (100% acetonitrile with 0.1% formic acid) for 4 min, and finally, the gradient returned to 2% solvent B for 20 min.

Xcaliber software version 4.4 was utilized for MS data collection. The Orbitrap analyzer scanned precursor ions within the mass range of 350-1800 m/z, achieving a resolution of 60,000 at m/z 200

2.10. Statistical analysis

All data underwent statistical analysis using GraphPad Prism 5.0 (GraphPad Software) and expressed as Mean with standard error of the mean (SEM). Statistical significance between groups was determined using one-way analysis of variance (ANOVA) followed by Dunnett's multiple comparisons post-hoc tests, with significance set at P value <0.05. GO analysis used the Database for Annotation, Visualization, and Integrated Discovery (DAVID), with a significance set at P <0.001.

3. Results

3.1. Characterization of C2C12 exosomes

To characterize exosomes isolated from myoblasts under serum starvation conditions, C2C12 MDE was purified under these conditions. Verifying MDE characterization involved calculating exosome size using NTA morphology via electron microscopy (EM) and the presence of exosome-specific proteins, including TSG101, Alix, and HSP70 [42, 43], using western blotting (WB). Furthermore, to validate the uptake of DiI-labeled exosomes by myoblasts, exosomes were labeled with DiI and observed using a fluorescence microscope. Alix and TSG101, known to assist in the formation of multivesicular bodies

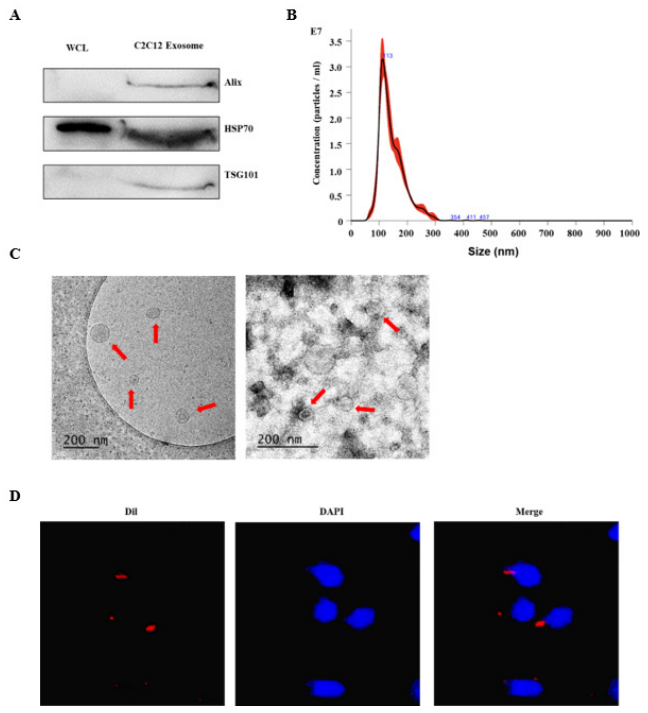

Fig. 1. Characterization of exosomes. (A) Western blot analysis shows the presence of exosome markers TSG101, Alix, and HSP70. (B) Nanoparticle tracking analysis (NTA) for quantifying the size of C2C12 myoblast exosomes. Concentration/size graph for exosomes. Size means 144.8 +/- 2.1. nm. (C) Left image: Cryo-electron microscopy (cryo-EM) and Right image: Transmission electron microscopy (TEM) images of exosomes (scale bars, 200 nm). (D) Exosomes labeled with DiI and C2C12 myoblasts nuclei stained with DAPI.

within endosomes [44], were found to be highly expressed during whole cell lysis (WCL). HSP70, known for its specific role when transported by exosomes [45], showed an equal expression level as WCL (Figure 1A). The average size of the purified exosomes, measured via NTA, was determined as 144.8 +/- 2.1 nm, falling within the typical size range of 30–150 nm [30], characteristic of exosomes (Figure 1B). Exosomes exhibit a lipid bilayer structure, as confirmed through TEM and Cryo-EM imaging (Figure 1C). Upon staining myoblast nuclei with DAPI and treating them with DiI-labeled exosomes, the exosomes were taken up by myoblasts. (Figure 1D), confirming their ability to enter and affect myoblasts.

3.2. Myoblasts-derived exosome enhanced cell viability

Serum starvation inhibited myoblast growth and induced cell death. [46] To validate the efficacy of exosomes secreted under these conditions, serum-starved MDEs were administered to C2C12 myoblasts, followed by a CCK-8 assay to assess cell viability. The results showed a dose-dependent increase in cell viability following exosome treatment under serum starvation (SF) and normal conditions. The increase in cell viability was significantly higher in the exosome-treated group under SF conditions than in normal conditions. At a concentration of 20 ug/ml, a significant increase of 63% was observed in cell viability under SF and 58% in the control group (COM) (Figure 2A, 2B). As cell viability increased, alterations in cell cycle and proliferation were investigated through cell counting and PI staining. While cell cycle changes were not significant in the exosome-treated group (Figure 2C), a notable increase in the number of viable cells was observed after exosome treatment under SF conditions (Figure 2D, 2E). This finding suggests that MDEs purified under serum-starvation conditions can affect cell survival, indicating their potential to protect and maintain myoblast numbers for self-regeneration during cell death conditions.

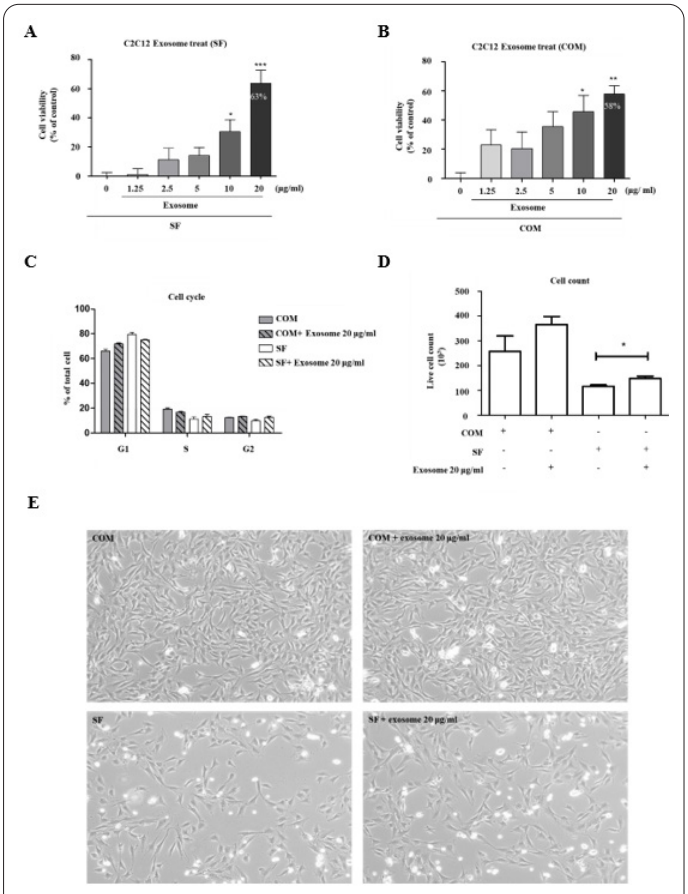

Fig. 2. Effects of C2C12 exosomes on cell proliferation. (A, B) Cell viability was assessed using a CCK-8 assay in the presence of COM and SF. (C) Analysis of cell cycle effects of exosomes on C2C12 via PI staining. (D, E) Representative images of treated cells and cell count (n=3).

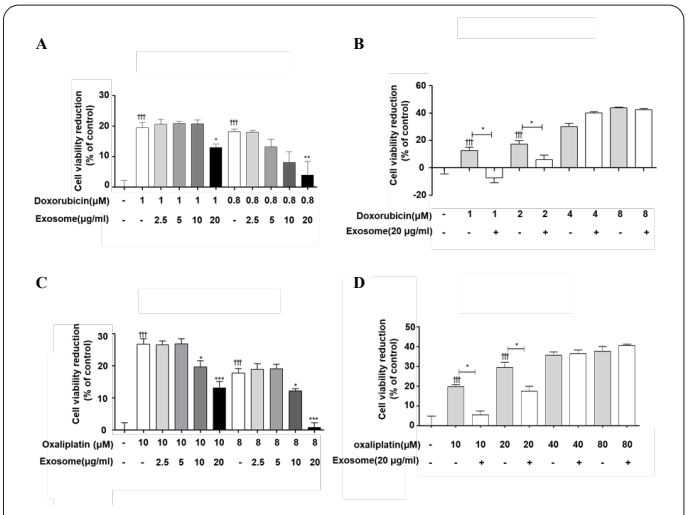

Fig. 3. Effect of C2C12 exosomes on anticancer drugs. This figure illustrates the effect of co-treatment with anticancer drugs and exosomes on myoblast cell viability. The exosome-mediated efficacy of anticancer agents has been confirmed up to a certain concentration. The data presented are the mean ± S.E.M of three independent experiments. Statistical significance levels are denoted as $^{*}p < 0.05$, $^{**}p < 0.01$, $^{***}p < 0.001$, indicating a comparison between the anticancer drug monotherapy groups and the exosome treatment group.

3.3. MDE restored myoblast cell viability reduction caused by anticancer drug toxicity

Given the observed enhancement in cell viability and survival with MDE treatment under cell death conditions, a CCK-8 assay was conducted to verify the effectiveness of MDE treatment in suppressing muscle toxicity caused by the anticancer drugs DOX and platinum-based OXA. [47] Using the SF-treated group as a control (0% cell viability), the results were expressed as a percentage reduction in cell viability. At a concentration of 1 μM, DOX treatment significantly reduced cell viability by an average of 19.4%, which decreased by 6.4% with simultaneous treatment of 20 ug/ml of MDEs. The efficacy of exosomes in mitigating DOX-induced cell viability reduction was observed up to a 2-μM treatment (Figure 3A, 3B). For OXA, significant cell viability decreases of 26% at 10 μM and 17% at 8 μM, compared to the control (SF), were observed. When exosomes were treated simultaneously with 10 μM OXA, the reduction in cell viability was reversed by 7.1% for 10 μg/ml exosomes and 13.6% for 20 μg/ml exosomes. In the OXA 8 μM treatment group, exosome treatment increased cell viability by 5.6% (10 μg/ml) and 17% (20 μg/ml), respectively, confirming that exosome treatment restored the reduction in cell viability of myoblasts via the anticancer drug. The efficacy of exosomes against OXA was highest at 10 μM and showed no effectiveness beyond 40 μM. (Figure 3C, 3D). These findings suggest that MDEs can restore the cell viability reduction caused by DOX and OXA treatments when administered at concentrations above 20 μg/ml. This suggests the potential of MDEs to mitigate muscle toxicity side effects of chemotherapy.

3.4. Proteomic analysis of MDEs

To identify the active substances within the exosomes, MDEs were characterized using RP-nano LC-ESI-MS/MS. After confirming the presence of proteins within the exosomes, 7,370 protein IDs were detected. Applying a Sequest HT score >10 and requiring at least two unique peptides, 1,074 protein IDs were identified. Corresponding gene IDs were obtained, and genes related to muscle differentiation were analyzed using the DAVID. The genes were categorized using commonly accepted GO terms related to molecular function, cellular components, and molecular biological functions, with a significance level of $p<0.001$. The GO analysis revealed several elements essential for cell growth, such as cell cycle and ATP (Figure 4A – 4C). Kyoto Encyclopedia of Genes and Genomes (KEGG) pathway analysis revealed significant genes related to metabolic pathways, such as the pyruvate cycle, which is directly related to cellular energy metabolism (Figure 4D). Overall, the classification of genes related to proteins within the MDEs indicated their involvement in multiple factors influencing cellular metabolic activities.

4. Discussion

Exosome signaling stimulates cell metabolism, reflecting the functional characteristics of the parent cells. Moreover, these characteristics are determined by the exosome contents. [48] MDEs were isolated under serum starvation conditions in this study, a scenario known to induce apoptosis in myoblasts. [40] Findings from this study show a significant increase in cell count and viability, especially during anti-cancer drug treatment. Furthermore, proteomic analysis of MDEs secreted under cell death conditions revealed the presence of proteins related to cell metabolism and survival. Therefore, exosomes from myoblasts under cell death conditions can serve as therapeutic agents to reduce muscle toxicity induced by anticancer drugs. Further research is needed to determine the effect of MDEs on myocytes or myotubes in the context of muscle toxicity. This will enable the confirmation of the muscle-protective function of exosomes secreted from myoblasts.

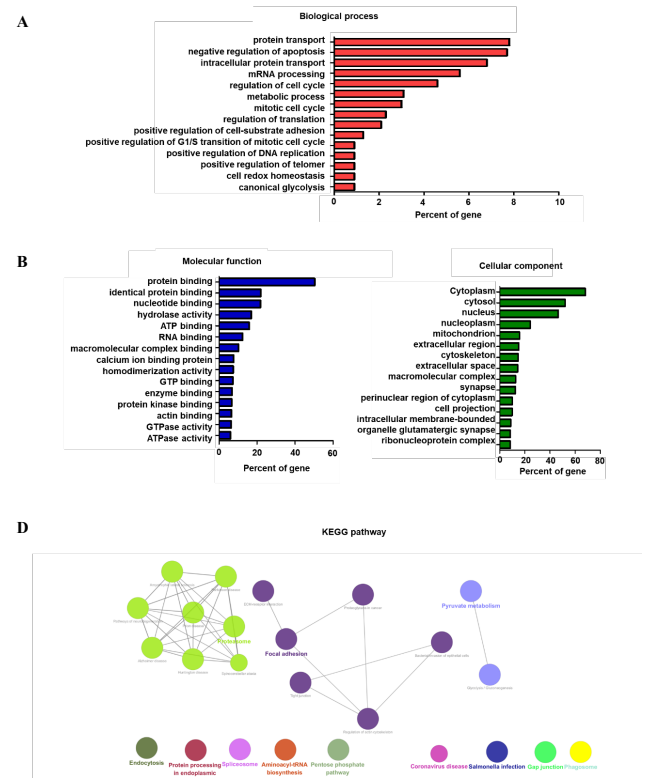

Fig. 4. Proteomic analysis of MDEs. This figure depicts the analysis of shared contents within cancer cell exosomes using DAVID. Gene ontology (GO) was categorized into biological process, molecular function, cellular component (A, B, C), and related KEGG pathway analysis (D).

Chemotherapy is the most prevalent treatment for cancer. However, these drugs can also affect normal cells, leading to severe side effects. [49] This study showed that chemotherapy drugs such as DOX and OXA restored cell viability. This suggests the possibility of protecting the activity of myoblast exosomes, thereby preventing cell death, and enhancing myoblast activity to accelerate muscle regeneration. Further research is necessary to uncover the specific mechanisms through which MDEs increase cell viability.

5. Conclusion

MDEs purified under serum starvation conditions reverse the reduction in cell viability caused by chemotherapeutic drugs. While further research is needed, these results indicate the potential to prevent muscle toxicity associated with cancer treatment

Conflict of interests

The authors declare that they have no conflict of interest The author has no conflicts with any step of the article preparation.

Consent for publications

The author read and approved the final manuscript for publication.

Ethics approval and consent to participate

No human or animals were used in the present research.

Informed consent

The authors declare that no patients were used in this study.

Availability of data and material

The data that support the findings of this study are available from the corresponding author upon reasonable request

Authors' contributions

Sang Bum Kim: Research design and supervision; Woojin Lee: Perform all laboratory procedures, Euijin Sohn: Provided support for the analysis

Funding

This work was supported by the National Research Foundation of Korea (NRF) Grant funded by the Korean Government (MSIT) (Grant Nos. 2022R1C1C1013481).

References

1. Fearon K, Strasser F, Anker SD, Bosaeus I, Bruera E, Fainsinger RL, Jatoi A, Loprinzi C, MacDonald N, Mantovani G, Davis M, Muscaritoli M, Ottery F, Radbruch L, Ravasco P, Walsh D, Wilcock A, Kaasa S, Baracos VE (2011) Definition and classification of cancer cachexia: an international consensus. Lancet Oncol 12 (5): 489-495. doi: 10.1016/S1470-2045(10)70218-7
2. Tijerina AJ (2004) The biochemical basis of metabolism in

cancer cachexia. Dimens Crit Care Nurs 23 (6): 237-243. doi: 10.1097/00003465-200411000-00001
3. WARREN S (1932) The immediate causes of death in cancer. Am J Med Sci 184 (5): 610-615.
4. Muscaritoli M, Anker SD, Argilés J, Aversa Z, Bauer JM, Biolo G, Boirie Y, Bosaeus I, Cederholm T, Costelli P, Fearon KC, Laviano A, Maggio M, Rossi Fanelli F, Schneider SM, Schols A, Sieber CC (2010) Consensus definition of sarcopenia, cachexia and pre-cachexia: joint document elaborated by Special Interest Groups (SIG) "cachexia-anorexia in chronic wasting diseases" and "nutrition in geriatrics". Clin Nutr 29 (2): 154-159. doi: 10.1016/j.clnu.2009.12.004
5. Martin L, Senesse P, Gioulbasanis I, Antoun S, Bozzetti F, Deans C, Strasser F, Thoresen L, Jagoe RT, Chasen M, Lundholm K, Bosaeus I, Fearon KH, Baracos VE (2014) Diagnostic Criteria for the Classification of Cancer-Associated Weight Loss. J Clin Oncol 33 (1): 90-99. doi: 10.1200/JCO.2014.56.1894
6. Johns N, Stephens NA, Fearon KC (2013) Muscle wasting in cancer. Int J Biochem Cell Biol 45 (10): 2215-2229. doi: 10.1016/j.biocel.2013.05.032
7. Sandri M (2016) Protein breakdown in cancer cachexia. Seminars Cell Develop Biol 54: 11-19. doi: https://doi.org/10.1016/j.semcdb.2015.11.002
8. Coletti D (2018) Chemotherapy-induced muscle wasting: an update. Eur J Transl Myol 28 (2): 7587. doi: 10.4081/ejtm.2018.7587
9. Voorwerk L, Slagter M, Horlings HM, Sikorska K, van de Vijver KK, de Maaker M, Nederlof I, Kluin RJC, Warren S, Ong S, Wiersma TG, Russell NS, Lalezari F, Schouten PC, Bakker NAM, Ketelaars SLC, Peters D, Lange CAH, van Werkhoven E, van Tinteren H, Mandjes IAM, Kemper I, Onderwater S, Chalabi M, Wilgenhof S, Haanen J, Salgado R, de Visser KE, Sonke GS, Wessels LFA, Linn SC, Schumacher TN, Blank CU, Kok M (2019) Immune induction strategies in metastatic triple-negative breast cancer to enhance the sensitivity to PD-1 blockade: the TONIC trial. Nat Med 25 (6): 920-928. doi: 10.1038/s41591-019-0432-4
10. Carvalho C, Santos RX, Cardoso S, Correia S, Oliveira PJ, Santos MS, Moreira PI (2009) Doxorubicin: The Good, the Bad and the Ugly Effect. Curr Med Chem 16 (25): 3267-3285. doi: 10.2174/092986709788803312
11. Cheung KG, Cole LK, Xiang B, Chen K, Ma X, Myal Y, Hatch GM, Tong Q, Dolinsky VW (2015) Sirtuin-3 (SIRT3) Protein Attenuates Doxorubicin-induced Oxidative Stress and Improves Mitochondrial Respiration in H9c2 Cardiomyocytes. J Biol Chem 290 (17): 10981-10993. doi: 10.1074/jbc.M114.607960
12. Renu K, V GA, P BT, Arunachalam S (2018) Molecular mechanism of doxorubicin-induced cardiomyopathy - An update. Eur J Pharmacol 818: 241-253. doi: 10.1016/j.ejphar.2017.10.043
13. Gagliardi PA, Dobrzyński M, Jacques M-A, Dessauges C, Ender P, Blum Y, Hughes RM, Cohen AR, Pertz O (2021) Collective ERK/Akt activity waves orchestrate epithelial homeostasis by driving apoptosis-induced survival. Dev Cell 56 (12): 1712-1726.e1716. doi: 10.1016/j.devcel.2021.05.007
14. Misset JL (1998) Oxaliplatin in practice. Br J Cancer 77 (4): 4-7. doi: 10.1038/bjc.1998.428
15. Raymond E, Faivre S, Woynarowski JM, Chaney SG (1998) Oxaliplatin: mechanism of action and antineoplastic activity. Seminars Oncol 25 (2 Suppl 5): 4-12. doi:
16. Raymond E, Faivre S, Chaney S, Woynarowski J, Cvitkovic E (2002) Cellular and Molecular Pharmacology of Oxaliplatin1. Molecular Cancer Therap 1 (3): 227-235. doi:
17. E. Raymond SGC, A. Taamma, E. Cvitkovic (1998) Oxaliplatin: A review of preclinical and clinical studies. Annal Oncol 9(10): 1053-1071. doi: 10.1023/A:1008213732429
18. Martinez-Balibrea E, Martinez-Cardus A, Gines A, Ruiz de Porras V, Moutinho C, Layos L, Manzano JL, Buges C, Bystrup S, Esteller M, Abad A (2015) Tumor-Related Molecular Mechanisms of Oxaliplatin Resistance. Mol Cancer Ther 14 (8): 1767-1776. doi: 10.1158/1535-7163.MCT-14-0636
19. Lees JG, Abdulla M, Barkl-Luke ME, Livni L, Keating BA, Hayes J, Fiore NT, Park SB, Moalem-Taylor G, Goldstein D (2021) Effect of exercise on neuromuscular toxicity in oxaliplatin-treated mice. Muscle Nerve 64 (2): 225-234. doi: 10.1002/mus.27329
20. Feather CE, Lees JG, Makker PGS, Goldstein D, Kwok JB, Moalem-Taylor G, Polly P (2018) Oxaliplatin induces muscle loss and muscle-specific molecular changes in Mice. Muscle Nerve 57 (4): 650-658. doi: 10.1002/mus.25966
21. Hiensch AE, Bolam KA, Mijwel S, Jeneson JAL, Huitema ADR, Kranenburg O, van der Wall E, Rundqvist H, Wengstrom Y, May AM (2020) Doxorubicin-induced skeletal muscle atrophy: Elucidating the underlying molecular pathways. Acta Physiol (Oxf) 229 (2): e13400. doi: 10.1111/apha.13400
22. Powers SK, Duarte JA, Le Nguyen B, Hyatt H (2019) Endurance exercise protects skeletal muscle against both doxorubicin-induced and inactivity-induced muscle wasting. Pflugers Arch 471 (3): 441-453. doi: 10.1007/s00424-018-2227-8
23. Huang SC, Wu JF, Saovieng S, Chien WH, Hsu MF, Li XF, Lee SD, Huang CY, Huang CY, Kuo CH (2017) Doxorubicin inhibits muscle inflammation after eccentric exercise. J Cachexia Sarcopenia Muscle 8 (2): 277-284. doi: 10.1002/jcsm.12148
24. Vaughan VC, Martin P, Lewandowski PA (2013) Cancer cachexia: impact, mechanisms and emerging treatments. J Cachexia Sarcopenia Muscle 4 (2): 95-109. doi: 10.1007/s13539-012-0087-1
25. Belizario JE, Fontes-Oliveira CC, Borges JP, Kashiabara JA, Vannier E (2016) Skeletal muscle wasting and renewal: a pivotal role of myokine IL-6. Springerplus 5: 619. doi: 10.1186/s40064-016-2197-2
26. von Haehling S, Anker SD (2014) Prevalence, incidence and clinical impact of cachexia: facts and numbers-update 2014. J Cachexia Sarcopenia Muscle 5 (4): 261-263. doi: 10.1007/s13539-014-0164-8
27. Ji S, Ma P, Cao X, Wang J, Yu X, Luo X, Lu J, Hou W, Zhang Z, Yan Y, Dong Y, Wang H (2022) Myoblast-derived exosomes promote the repair and regeneration of injured skeletal muscle in mice. FEBS Open Bio 12 (12): 2213-2226. doi: 10.1002/2211-5463.13504
28. Wang Z, Yang J, Sun X, Sun X, Yang G, Shi X (2023) Exosome-mediated regulatory mechanisms in skeletal muscle: a narrative review. J Zhejiang Univ Sci B 24 (1): 1-14. doi: 10.1631/jzus.B2200243
29. Motohashi N, Asakura A (2014) Muscle satellite cell heterogeneity and self-renewal. Front Cell Dev Biol 2: 1. doi: 10.3389/fcell.2014.00001
30. Yanez-Mo M, Siljander PR, Andreu Z, Zavec AB, Borras FE, Buzas EI, Buzas K, Casal E, Cappello F, Carvalho J, Colas E, Cordeiro-da Silva A, Fais S, Falcon-Perez JM, Ghobrial IM, Giebel B, Gimona M, Graner M, Gursel I, Gursel M, Heegaard NH, Hendrix A, Kierulf P, Kokubun K, Kosanovic M, Kralj-Iglic V, Kramer-Albers EM, Laitinen S, Lasser C, Lener T, Ligeti E, Line A, Lipps G, Llorente A, Lotvall J, Mancek-Keber M, Marcilla A, Mittelbrunn M, Nazarenko I, Nolte-'t Hoen EN, Nyman TA, O'Driscoll L, Olivan M, Oliveira C, Pallinger E, Del Portillo HA, Reventos J, Rigau M, Rohde E, Sammar M, Sanchez-Madrid F, Santarem N, Schallmoser K, Ostenfeld MS, Stoorvogel W, Stukelj R, Van der Grein SG, Vasconcelos MH, Wauben MH, De Wever O (2015) Biological properties of extracellular vesicles and their physiological functions. J Extracell Vesicles 4: 27066. doi: 10.3402/jev.v4.27066

31. Diaz G, Wolfe LM, Kruh-Garcia NA, Dobos KM (2016) Changes in the Membrane-Associated Proteins of Exosomes Released from Human Macrophages after Mycobacterium tuberculosis Infection. Sci Rep 6: 37975. doi: 10.1038/srep37975
32. Kruh-Garcia NA, Wolfe LM, Chaisson LH, Worodria WO, Nahid P, Schorey JS, Davis JL, Dobos KM (2014) Detection of Mycobacterium tuberculosis peptides in the exosomes of patients with active and latent M. tuberculosis infection using MRM-MS. PLoS One 9 (7): e103811. doi: 10.1371/journal.pone.0103811
33. Patel GK, Khan MA, Zubair H, Srivastava SK, Khushman M, Singh S, Singh AP (2019) Comparative analysis of exosome isolation methods using culture supernatant for optimum yield, purity and downstream applications. Sci Rep 9 (1): 5335. doi: 10.1038/s41598-019-41800-2
34. Zhang Y, Liu Y, Liu H, Tang WH (2019) Exosomes: biogenesis, biologic function and clinical potential. Cell Biosci 9: 19. doi: 10.1186/s13578-019-0282-2
35. Luo ZW, Sun YY, Lin JR, Qi BJ, Chen JW (2021) Exosomes derived from inflammatory myoblasts promote M1 polarization and break the balance of myoblast proliferation/differentiation. World J Stem Cells 13 (11): 1762-1782. doi: 10.4252/wjsc.v13.i11.1762
36. Maji S, Chaudhary P, Akopova I, Nguyen PM, Hare RJ, Gryczynski I, Vishwanatha JK (2017) Exosomal Annexin II Promotes Angiogenesis and Breast Cancer Metastasis. Mol Cancer Res 15 (1): 93-105. doi: 10.1158/1541-7786.Mcr-16-0163
37. Zhou X, Yan T, Huang C, Xu Z, Wang L, Jiang E, Wang H, Chen Y, Liu K, Shao Z, Shang Z (2018) Melanoma cell-secreted exosomal miR-155-5p induce proangiogenic switch of cancer-associated fibroblasts via SOCS1/JAK2/STAT3 signaling pathway. J Exp Clin Cancer Res 37 (1): 242. doi: 10.1186/s13046-018-0911-3
38. Chen J, Chopp M (2018) Exosome Therapy for Stroke. Stroke 49 (5): 1083-1090. doi: 10.1161/STROKEAHA.117.018292
39. van der Pol E, Boing AN, Harrison P, Sturk A, Nieuwland R (2012) Classification, functions, and clinical relevance of extracellular vesicles. Pharmacol Rev 64 (3): 676-705. doi: 10.1124/pr.112.005983
40. Wang Y, Always SE (2007) N-CADHERIN PROTECTS C2C12 MYOBLASTS FROM SERUM-STARVATION-INDUCED APOPTOSIS. The FASEB Journal 21 (6): A1343-A1343. doi: https://doi.org/10.1096/fasebj.21.6.A1343
41. Kim H-u, Bharda AV, Moon JC, Jeoung D, Chung JM, Jung HS (2021) Microscopic studies on severing properties of actin-binding protein: its potential use in therapeutic treatment of actin-rich inclusions. Journal of Analytical Science and Technology 12 (1). doi: 10.1186/s40543-021-00305-2
42. Valcz G, Galamb O, Krenács T, Spisák S, Kalmár A, Patai ÁV, Wichmann B, Dede K, Tulassay Z, Molnár B (2016) Exosomes in colorectal carcinoma formation: ALIX under the magnifying glass. Modern Pathology 29 (8): 928-938. doi: https://doi.org/10.1038/modpathol.2016.72
43. Li S, Li X, Yang S, Pi H, Li Z, Yao P, Zhang Q, Wang Q, Shen P, Li X, Ji J (2021) Proteomic Landscape of Exosomes Reveals the Functional Contributions of CD151 in Triple-Negative Breast Cancer. Mol Cell Proteomics 20: 100121. doi: 10.1016/j.mcpro.2021.100121
44. Morita E, Sandrin V, Chung H-Y, Morham SG, Gygi SP, Rodesch CK, Sundquist WI (2007) Human ESCRT and ALIX proteins interact with proteins of the midbody and function in cytokinesis. EMBO J 26 (19): 4215-4227. doi: https://doi.org/10.1038/sj.emboj.7601850
45. Komarova EY, Suezov RV, Nikotina AD, Aksenov ND, Garaeva LA, Shtam TA, Zhakhov AV, Martynova MG, Bystrova OA, Istomina MS, Ischenko AM, Margulis BA, Guzhova IV (2021) Hsp70-containing extracellular vesicles are capable of activating of adaptive immunity in models of mouse melanoma and colon carcinoma. Sci Rep 11 (1): 21314. doi: 10.1038/s41598-021-00734-4
46. Jang M, Scheffold J, Røst LM, Cheon H, Bruheim P (2022) Serum-free cultures of C2C12 cells show different muscle phenotypes which can be estimated by metabolic profiling. Sci Rep 12 (1). doi: 10.1038/s41598-022-04804-z
47. Stefanetti RJ, Lamon S, Wallace M, Vendelbo MH, Russell AP, Vissing K (2015) Regulation of ubiquitin proteasome pathway molecular markers in response to endurance and resistance exercise and training. Pflugers Arch 467 (7): 1523-1537. doi: 10.1007/s00424-014-1587-y
48. Kalluri R, LeBleu VS (2020) The biology, function, and biomedical applications of exosomes. Science 367 (6478). doi: 10.1126/science.aau6977
49. McKnight JA (2003) Principles of chemotherapy. Clinical Techniques in Small Animal Practice 18 (2): 67-72. doi: https://doi.org/10.1053/svms.2003.36617